

A PROBLEM CLASS WITH COMBINED ARCHITECTURE, PLANT, AND CONTROL DESIGN APPLIED TO VEHICLE SUSPENSIONS

Daniel R. Herber*, James T. Allison

University of Illinois at Urbana-Champaign
Industrial & Enterprise Systems Engineering
Urbana, IL 61801

Email: {[herber1](mailto:herber1@illinois.edu), [jtalliso](mailto:jtalliso@illinois.edu)}@illinois.edu

Abstract

Here we describe a problem class with combined architecture, plant, and control design for dynamic engineering systems. The design problem class is characterized by architectures comprised of linear physical elements and nested co-design optimization problems employing linear-quadratic dynamic optimization. The select problem class leverages a number of existing theory and tools and is particularly effective due to the symbiosis between labeled graph representations of architectures, dynamic models constructed from linear physical elements, linear-quadratic dynamic optimization, and the nested co-design solution strategy. A vehicle suspension case study is investigated and a specifically constructed architecture, plant, and control design problem is described. The result was the automated generation and co-design problem evaluation of 4,374 unique suspension architectures. The results demonstrate that changes to the vehicle suspension architecture can result in improved performance, but at the cost of increased mechanical complexity. Furthermore, the case study highlights a number of challenges associated with finding solutions to the considered class of design problems. One such challenge is the requirement to use simplified design problem elements/models; thus, the goal of these early-stage studies are to identify new architectures that are worth investigating more deeply. The results of higher-fidelity studies on a subset of high-performance architectures can then be used to select a final system architecture. In many aspects, the described problem class is the simplest case applicable to graph-representable, dynamic engineering systems.

*Corresponding author.

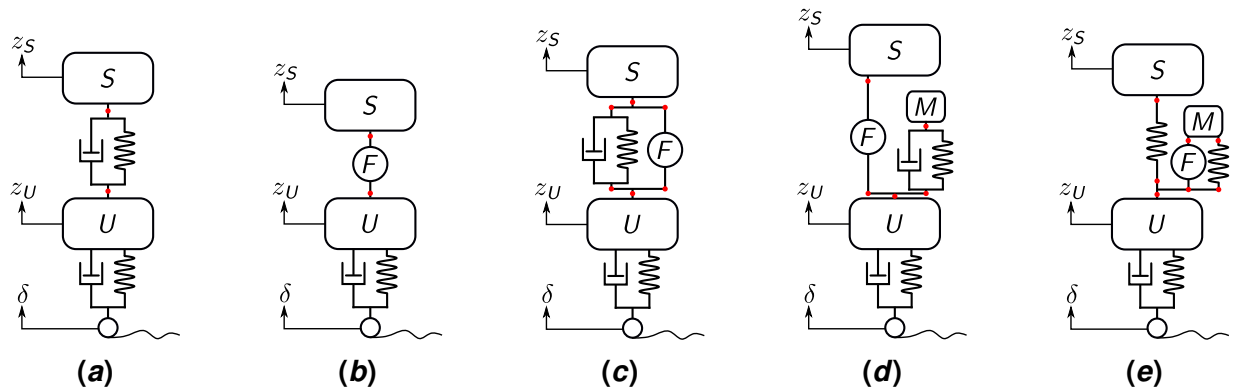


Fig. 1 Some vehicle suspension architectures: (a) canonical passive [4, 6]; (b) pure active [2, 3]; (c) canonical active [5, 15–18]; (d) active with dynamic absorber [2, 3]; (e) an alternative active architecture.

1 INTRODUCTION

The design of vehicle suspensions has been of considerable interest ever since the invention of the automobile. A suspension transfers forces in the system to provide a smooth ride for the passenger and good handling characteristics among other objectives. Fundamentally, it is a type of vibration isolator [1–3]. Different types of suspensions can typically be classified into the three categories of passive [1–11], semi-active [3, 12–14], or active [2, 3, 15–18] depending on the external energy flow into the system. There has been considerable research interest in analyzing and optimizing all types of suspensions, particularly utilizing tools from dynamics and controls. However, much of this research has focused on a select few canonical suspensions such as the ones shown in Figs. 1(a)–1(d). Here we will consider architecture¹ changes in the suspensions, i.e., different components connected in new ways such as the suspension shown in Fig. 1(e). Realizing new architectures is commonly presented as synthesis. There have been many developments in the synthesis of passive vehicle suspensions [7–11], but less attention given to active systems.

In one-dimensional suspension systems, an unsprung mass U with position z_U is connected to the road profile δ , typically through a parallel spring and damper that captures the tire dynamics. There is also a sprung mass S with position z_S . There will exist some mechanical path (known as the suspension) between S and U . The performance of a suspension system is then evaluated by observing the dynamic behavior of both the sprung and unsprung masses with respect to road profile variations, and several candidate performance metrics based on this behavior exist. This is a commonly-used simplified treatment of the kinematics, but can only capture the performance metrics to certain degree of accuracy.

In addition to potential architecture design changes, we will consider design elements in both the physical (or plant) and control design domains. Here plant variables are time-independent quantities that relate to the physical embodiment of the suspension such as the stiffness of the springs or the damping coefficient for the dampers. The control design is associated with the actuator force trajectories (e.g., the force produced by component F in Fig. 1(b)) which are time-varying inputs to the system that can regulate the dynamic behavior of the system.

This level of design freedom leads to a complex, challenging design problem that is typically not treated in a systematic fashion in engineering design practice. Due to the large scope of the proposed design study, many simplifying assumptions must be made to keep the problem tractable, but we need a certain level of veracity such that it is still possible to reveal the desired design insights. This motivates

¹Changes in the topology, configuration, or network are often-used, alternative terms used to describe the same type of design decision.

the use of a particular problem class of combined architecture, plant, and control problems that has sufficiently developed theory and tools that can be leveraged to provide relatively efficient solutions. This design problem class selected here is characterized by architectures comprised of *linear physical elements* (LPEs) and nested co-design optimization problems employing *linear-quadratic dynamic optimization* (LQDO); these concepts operate collectively, facilitating a relatively efficient solution strategy. The problem class will be fully defined in the following section.

It has been observed by suspension design experts that even simple suspension models and studies have had a “profound impact on the practical implementations some 15–20 years later [3]”. In addition, suspension design problems with similar design fidelity have proven to be an interesting area for research in co-design (or combined plant and control design) [15–17]. These co-design studies considered a single architecture, which is typically the canonical active system in Fig. 1(c). It is important to note that the purpose of the early-stage studies proposed in this article is not to supplant the detailed, rigorous previous research, but rather seeks to identify new architectures that could be investigated in the same level of detail that the few canonical architectures have received.

The contributions of this article are 1) the description of a problem class with combined architecture, plant, and control design with structure that can be exploited; 2) a trilevel solution strategy for problems in this class combining a number of solution techniques; and 3) a engineering case study on the design of vehicle suspensions illustrating the problem class. The remainder of this article is organized as follows. Section 2 discusses some important considerations when dealing with combined architecture, plant, and control design problems. Section 3 outlines the considered problem class and proposed solution approach. Section 4 describes the set of candidate vehicle suspension architectures. Section 5 details the combined architecture, plant, and control vehicle suspension design problem formulation. Section 6 presents the results of the case study and, Sec. 7 continues the discussion on the problem class, solution methods, and vehicle suspension design problem. Finally, Sec. 8 provides the conclusions.

2 CONSIDERATIONS FOR A PROBLEM CLASS WITH COMBINED ARCHITECTURE, PLANT, AND CONTROL DESIGN

Since the proposed level of design freedom leads to a complex, challenging design problem, we first list some important considerations. Addressing these comments will eventually facilitate the study of different vehicle suspensions.

1. Meaningful candidate architectures can readily be generated; this is typically handled by defining suitable components that can be connected together in meaningful ways.
2. Given some representation of an architecture, a model can be automatically constructed that captures its dynamic behavior.
3. The components are defined at an acceptable level with respect to modeling and design while preferring computationally inexpensive embodiments.
4. The evaluation of a candidate architecture’s performance is possible and efficient.
5. Since we are considering dynamic systems, it is preferred that the generated model provides an explicit state derivative function to facilitate the use of a variety of solution methods.

Now, we can discuss how systems with LPEs, LQDO, and nested co-design at least partially address these considerations.

2.1 Linear Physical Elements

A useful framework for describing LPEs is bond graph modeling with power port nodes (or simply power nodes) [19]. Power nodes are characterized by constitutive parameters and follow some constitutive relation (typically a fundamental physical law). They can be classified as source nodes (Se , Sf),

Table 1 Some bond graph modeling analogies.

Linear Mechanical				
Label	Intuitive	Topology Preserving	Electrical	Hydraulic
Se	Force	Velocity	Voltage	Pressure
Sf	Velocity	Force	Current	Volume
C	(Spring Constant) ⁻¹	Mass	Capacitance	Storage
I	Mass	(Spring Constant) ⁻¹	Inductance	Fluid Inductance
R	Damping Constant	(Damping Constant) ⁻¹	Resistance	Fluid Resistance

storage nodes (C , I), resistive nodes (R), reversible transducers (TF , GY), and junction nodes (0 , 1). Some analogies for these power nodes in different energy domains are listed in Table 1. An example of a TF (transformer) is a lever, gear, or hydraulic cylinder. The GY (gyrator) typically describes the conversion between energy domains, such as with an electrical DC motor or mass accelerometer. The 0 -junction is analogous to Kirchhoff's current law and the 1 -junction is analogous to the voltage law in electrical systems. With these elements, many (multi-domain) engineering systems with mechanical, electrical, hydraulic, magnetic, etc. elements can be modeled to some degree. For more details on bond graph modeling, see Refs. [19–21].

The key property for systems represented by bond graphs with linear time-invariant elements is that the equations of motion can be represented as a *linear descriptor model* [22,23]. If we denote the set of all constitutive parameters for a particular bond graph as \mathbf{p} , the dynamic model is of the form:

$$E(\mathbf{p})\dot{\boldsymbol{\xi}} = A(\mathbf{p})\boldsymbol{\xi} + B(\mathbf{p})\mathbf{s} \quad (1)$$

where $\boldsymbol{\xi}$ are the states, \mathbf{s} are the sources, E is the descriptor matrix, A is the state matrix, and B is the input matrix. The matrix E is invertible if there are no algebraic loops in the system [19, 22, 23]. Here we assume that all algebraic loops are appropriately removed (e.g., see Ref. [22] or the modeling approach used below) so that we have an explicit first-order ordinary differential equation (ODE).

We will also utilize the notation of outputs \mathbf{y} to capture certain dynamic quantities in the architecture. As long as the desired outputs (e.g., acceleration of S or position of the U) are a linear combination of the states and sources, then we can obtain a linear output equation in the standard state-space representation:

$$\mathbf{y} = C(\mathbf{p})\boldsymbol{\xi} + D(\mathbf{p})\mathbf{s} \quad (2)$$

where C is the output matrix and D is the feedthrough matrix.

Now, the architecture-related design decisions will include what power nodes to include in the system and their connections, satisfying consideration 1. Therefore, an architecture is a (bond) graph, and each architecture may have different \mathbf{p} -dependent matrix forms and states. Some of the constitutive parameters will be the plant design variables, such as the stiffness coefficient of the spring component. Hence, the matrices in Eqs. (1) and (2) will depend on both plant variables and any other fixed constitutive parameters, denoted \mathbf{p}_f . The control decisions will come in the form of certain source types. The sources may also be used to add various disturbances to the system. Since bond graph models and optimization with respect to constitutive parameters and source inputs are commonly accepted, we can satisfy consideration 3 to a certain degree.

Utilizing architectures consisting of LPEs permits the use of a number of available tools for automated model creation, which are needed to satisfy consideration 2. For general bond graph models, tools such as MODELICA [24] and MTT [25] are available. However, it was found to be challenging to obtain

Ref. [28] is what we define as the LQDO problem class.

2.3 Nested Co-Design Solution Strategy

Consider the following general co-design problem:

$$\begin{aligned} \min_{\mathbf{x}_p, \mathbf{x}_c} \quad & \Psi(\mathbf{x}_p, \mathbf{x}_c) & (4a) \\ \text{subject to:} \quad & \mathbf{g}_o(\mathbf{x}_p) \leq \mathbf{0}, \mathbf{g}_i(t, \mathbf{x}_p, \mathbf{x}_c) \leq \mathbf{0} & (4b) \end{aligned}$$

where \mathbf{x}_p are the plant variables, \mathbf{x}_c are the control variables, $\Psi(\cdot)$ is the general objective function, and \mathbf{g} represent general constraints. Constraints \mathbf{g}_o capture the time independent, plant-only constraints while \mathbf{g}_i captures all time, control, and state dependent constraints including the dynamics.

Two common methods for solving co-design problems are the simultaneous and nested solution strategies [15,29,30]. In the simultaneous approach, we seek a feasible minimizer while simultaneously modifying both \mathbf{x}_p and \mathbf{x}_c . To define the nested approach, we first consider the set of feasible control designs given candidate plant \mathbf{x}_p^\dagger with respect to \mathbf{g}_i :

$$\Omega_i(\mathbf{x}_p^\dagger) = \{ \mathbf{x}_c : \mathbf{g}_i(t, \mathbf{x}_p^\dagger, \mathbf{x}_c) \leq \mathbf{0} \} \quad (5)$$

Then the nested strategy proceeds through a two-level optimization scheme where an *outer loop* optimizes with respect to the plant variables and an *inner loop* optimizes with respect to the control variables for a given plant design:

$$\mathbf{x}_p^* = \arg \min_{\mathbf{x}_p} \{ \Psi(\mathbf{x}_p, \mathcal{I}(\mathbf{x}_p)) : \mathbf{g}_o(\mathbf{x}_p) \leq \mathbf{0} \} \quad (\text{outer}) \quad (6a)$$

$$\mathcal{I}(\mathbf{x}_p^\dagger) = \arg \min_{\mathbf{x}_c} \{ \Psi(\mathbf{x}_p^\dagger, \mathbf{x}_c) : \mathbf{x}_c \in \Omega_i(\mathbf{x}_p^\dagger) \} \quad (\text{inner}) \quad (6b)$$

where the mapping $\mathcal{I} : \mathbf{x}_p \mapsto \mathbf{x}_c$ must exist for all considered values of \mathbf{x}_p for the simultaneous and nested approaches to be equivalent [29,30].

The key advantage of the nested approach is that different optimization methods can be utilized in the inner/outer loops. Therefore, the partitioning of the inner/outer loops can be justified if there are efficient methods that cannot be leveraged using the simultaneous form. In fact, a co-design problem with LPEs and OLCs variables can be formed such that the inner-loop problem is an LQDO problem (and the simultaneous form would need to be at least bilinear). This is due to the fact that for fixed values of \mathbf{p} , Eq. (1) with invertible \mathbf{E} is in the appropriate form for Eq. (3c) in LQDO. A number of studies have shown the benefits of the nested strategy when an efficient inner-loop solution method is available [30–32], and utilizing nested co-design helps satisfy consideration 4. Additionally, since co-design problems are potentially nonconvex, we can now focus our global search efforts only in the outer loop with respect to the plant variables since the inner loop is convex.

3 PROBLEM CLASS DEFINITION AND SOLUTION APPROACH

We now will formally define the problem class of interest and the proposed solution approach.

3.1 Problem Class Definition

We would like to solve architecture design problems posed as combinatorial optimization problems of the following form:

$$\min_a \Psi = \Psi_a(a) + \Psi_d(\mathcal{X}_p(a), \mathcal{X}_c(a)) \quad (7a)$$

$$\text{subject to: } a \in \mathcal{F}_a \quad (7b)$$

where a is an architecture and \mathcal{F}_a is the set of feasible architectures. Ψ_a is the architecture-only objective function while Ψ_d is the general co-design objective function that includes dependence on the plant and control design. This dependence is represented by the mapping functions $\mathcal{X}_p : a \mapsto \mathbf{x}_p^*$ and $\mathcal{X}_c : a \mapsto \mathbf{u}^*$ between the architecture and the optimal plant and OLC design variables for a soon to be specified co-design problem. The fixed constitutive parameters \mathbf{p}_f may also depend on a and can be included in Ψ_d but are omitted for brevity.

A fair comparison between architecture candidates requires knowledge of the best possible performance for each candidate architecture. To determine the value of Ψ_d we must solve a suitable co-design problem of the following form:

$$\min_{\mathbf{x}_p^{(i)}, \mathbf{u}^{(i)}} \Psi_d = \int_{t_0}^{t_f} \mathcal{L}^{\mathcal{N}}(t, \mathbf{y}, \mathbf{x}_p^{(i)}) dt + \dots \quad (8a)$$

$$\mathcal{M}^{\mathcal{N}}(\mathbf{y}(t_0), \mathbf{y}(t_f), \mathbf{x}_p^{(i)}) \quad (8b)$$

$$\text{subject to: } \left[\dot{\boldsymbol{\xi}} = \mathbf{f}^{\mathcal{N}}(t, \boldsymbol{\xi}, \mathbf{u}, \mathbf{x}_p) \right]^{(i)} \quad (8c)$$

$$\mathbf{g}^{\mathcal{N}}(t, \mathbf{y}, \mathbf{x}_p^{(i)}) \leq \mathbf{0} \quad (8d)$$

$$\text{where: } \mathbf{y} = \mathbf{y}(t, \boldsymbol{\xi}^{(i)}, \mathbf{u}^{(i)}, \mathbf{x}_p^{(i)}) \quad (8e)$$

where \mathcal{L} is the running cost, \mathcal{M} is the terminal cost, \mathbf{f} is the explicit state derivative function, \mathbf{g} are the inequality constraints, $\square^{(i)}$ indicates a problem formulation element appropriate for the i th candidate architecture from Prob. (7), \mathbf{y} are the architecture-dependent outputs in Eq. (2), and the superscript \mathcal{N} indicates a particular problem class that the problem elements must be in. Here we consider \mathcal{N} as the LQDO-amenable co-design problem class based on the considerations in Sec. 2.

Definition 1. A co-design problem is said to be an LQDO-amenable co-design problem if for fixed values of \mathbf{x}_p , all problem elements are within the LQDO problem class in Sec. 2.2.

To ensure that Eq. (8c) satisfies these conditions, the models of the architectures must be constructed from LPEs (see Sec. 2.1). With the problem class defined, we can now describe the trilevel solution strategy.

3.2 A Trilevel Solution Approach

Consider the following definition of an optimal solution to a combinatorial optimization problem.

Definition 2. Solution $a^* \in \mathcal{F}_a$ is an optimum solution of Prob. (7) if $\Psi(a^*) \leq \Psi(a)$ for all $a \in \mathcal{F}_a$.

Unlike some combinatorial optimization problems, such as the traveling salesman, knapsack, assignment, or vertex coloring problems [33], there are limited exact or approximation algorithms that are suitable for the selected problem class. This might be due to the fact that although architectures are defined by graph-theoretic concepts, their performance is not. Until such solution approaches exist, the only way to guarantee that you find the optimal architecture is to evaluate all feasible architectures.

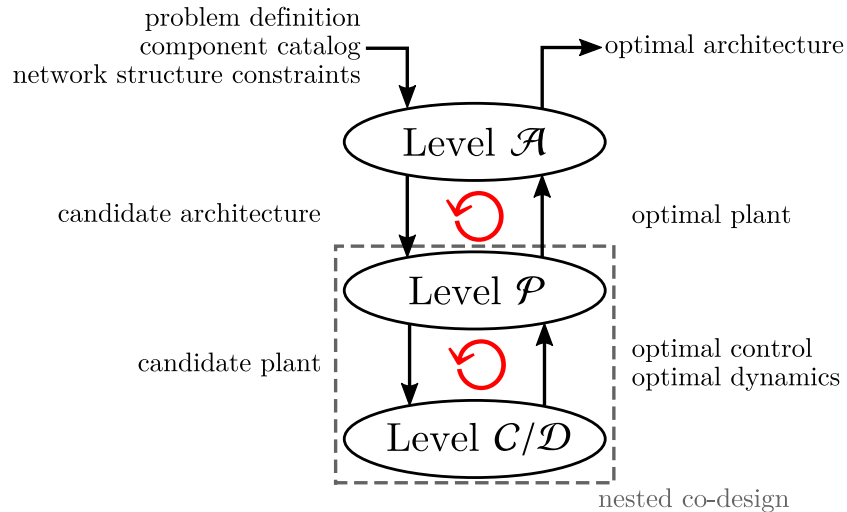


Fig. 3 The proposed trilevel solution strategy for combined architecture, plant, and control design of a dynamic system.

However, such an approach is only suitable for problems of a certain size, and this idea is discussed further in Sec. 7.

The proposed solution approach treats each design domain modularly to leverage existing theory and tools that provide relatively efficient solutions and address the aforementioned considerations. This leads to the trilevel solution approach, where each design domain is a level, and is illustrated in Fig. 3. Here, we term the combined architecture, plant, and control design problem as an \mathcal{APC} problem. Each one of the three levels is now described.

3.2.1 Architecture Design: Level \mathcal{A} .

The topmost level is responsible for taking the problem definition, a user-defined component catalog, and network structure constraints and providing candidate architectures for the other levels.

Here we will use undirected labeled graphs to represent candidate architectures [33, 34]. The different labels in the graphs will correspond to the power nodes in Sec. 2.1 or superelements (some subgraph of power nodes) [19–21, 28]. There is a strong resemblance between the equivalent bond graph or block-diagram model (such as a SIMSCAPE/SIMULINK model). For example, compare Figs. 2(a) and 2(b) for a specific suspension architecture. Some advantages of using a labeled graph representation are that labels can be used to represent a variety of concepts and existing graph theory and tools can be utilized.

Working with undirected labeled graphs, the brute-force generation procedure described in Ref. [34] will be used to produce an enumeration (or complete listing) of all the feasible architectures in the considered feasible space. This approach utilizes a perfect matching-inspired algorithm where all ports (or potential connections) of every component (or vertex in the graph) are connected to exactly one other port [34, 35]. In the worst case scenario, the growth of the number of graphs (architectures) is $(N - 1)!!$ where N is the total number of ports and $(\cdot)!!$ represents the double factorial function. However, this bound is extremely conservative as many of the generated graphs are isomorphic (not unique) or do not satisfy network structure constraints (NSCs). Satisfaction of all NSCs defines the feasibility for a particular graph and the set \mathcal{F}_a [34, 36]. Many enhancements to the original approach in Refs. [34, 37] have been made in Ref. [38], further leveraging the structure of the enumeration task and allowing reasonably large graph structure spaces to be enumerated.

The required information for this approach is the following designer-defined elements:

- C is the label sequence representing distinct component types

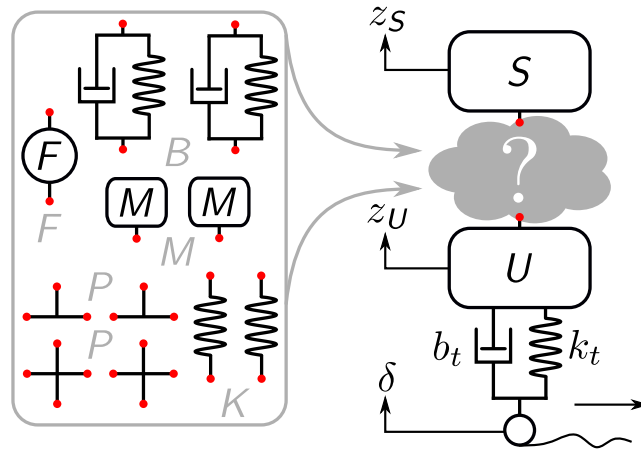


Fig. 4 Vehicle suspension architecture design domain.

- P is a vector indicating the number of ports for each component type
- (R_{\min}, R_{\max}) are a vectors indicating the minimum/maximum number of replicates for each component type; R is the collection of both vectors

The collection (C, R, P) is termed the component catalog.

3.2.2 Plant Design: Level \mathcal{P} .

The next level takes the candidate architecture and performs the outer-loop co-design tasks for the plant design [30]. The automated model generation procedure described in Sec. 2.1 and shown in Fig. 2 creates a suitable model. Then the appropriate optimization problem in the form of Prob. (6a) is automatically created and solved. Since this type of problem can be nonconvex (see Sec. A), global search algorithms are utilized to help improve the confidence of finding the true optimal solution.

3.2.3 Control Design and Dynamics: Level C/\mathcal{D} .

This deepest level takes the model and candidate plant and formulates the appropriate LQDO problem. Note that the number of times Level C/\mathcal{D} is solved is much greater than Level \mathcal{P} , which is also solved for many times in Level \mathcal{A} for different candidate architectures. Successfully solving a Level C/\mathcal{D} problem provides both the optimal control and dynamics, thus, providing a evaluation of Ψ_d . Here we will utilize the MATLAB code available at Ref. [39] for solving the LQDO problem using direct transcription methods [28]. The code utilizes a structure-based description of the optimization problem, which makes it relatively straightforward to handle a varying number of states and controls along with the output definitions [28].

4 SPECIFICATION OF THE CANDIDATE VEHICLE SUSPENSION ARCHITECTURES

Here we will use undirected labeled graphs to represent candidate vehicle suspension architectures as described in Sec. 3.2.1 [34].

4.1 Component Catalog Specification

The component catalog will be the similar to the one used in Refs. [34, 38]:

$$C = \{S U M K B F P P\} \quad (9a)$$

$$R_{\min} = \begin{bmatrix} 1 & 1 & 0 & 0 & 0 & 1 & 0 & 0 \end{bmatrix} \quad (9b)$$

$$R_{\max} = \begin{bmatrix} 1 & 1 & 2 & 2 & 2 & 1 & 2 & 2 \end{bmatrix} \quad (9c)$$

$$P = \begin{bmatrix} 1 & 1 & 1 & 2 & 2 & 2 & 3 & 4 \end{bmatrix} \quad (9d)$$

The region between S and U is termed the suspension strut [8, 10, 11] and is the location where the additional components may be included in the suspension system. The fixed arrangement of certain components in the problem is frequently called the template graph [28]. Both are represented in Fig. 4. Each of the component types fits within the bond graph modeling paradigm: $\{S, U, M\}$ are I -type storage nodes, K is a C -type storage node, B is a subsystem containing a spring and damper (R -type node) in parallel³ (see Fig. 4), and F is an $\mathcal{S}e$ -type effort source. The remaining component types represent 1 -junctions with differing numbers of ports.

The selection of the component types and their model was based on observations on the components that have been commonly used in different suspensions. The required components are (S, U, F) , so we are considering active suspensions only. The maximum number of replicates for the other component types was selected based on what is reasonable for enumeration as well as being able to explore a reasonable space of novel suspension architectures. Other template graphs have been considered including a predetermined static stiffness between S and U [9]. Another commonly considered component is the mechanical inerter (a 2-port, ungrounded mass component [7, 8, 10]). This component can be included in future component catalogs as it is a LPE.

4.2 Network Structure Constraints

All the NSCs for this problem are listed in Ref. [34]. Here we summarize only a few of the more important ones:

- Each included component must have unique edges in the graph (i.e., no multi-edges).
- A mechanical path between the U and S must be present and this path cannot only contain P -type components.
- Certain component types should not be connected together (e.g., $U - S$, $K - K$, or $P - P$).
- Only consider a specific ordering of the series connections because permuting them results in an equivalent model (e.g., $K - B$ and $B - K$ in series are physically equivalent).
- Component F must be connected to two different P except for the canonical active suspension to prevent some modeling issues (see Sec. 5.3), and this NSC could be removed when the internal positioning constraints are properly included.

4.3 Architecture Cost Metric

The architecture-only objective function term considered here is the sum of the additional physical components (i.e., all components except S , U , and P):

$$\Psi_a = w_a N_c = w_a (n_M + n_K + 2n_B + n_F) \quad (10)$$

³The additional spring is a ‘centering spring’ that ensures that all points in the suspension are determinate in the steady state [40].

where w_a is the weighting coefficient. This is just one metric for attempting to account for the complications that can occur from an increased mechanical complexity of the system (e.g., monetary cost, reliability, and other design challenges).

5 ARCHITECTURE-DEPENDENT CO-DESIGN PROBLEM

The co-design problem can be posed through the outputs, dynamics, objective, and constraints. The forms of these problem elements are consistent across the different candidate architectures, but their specific realization will be architecture dependent.

5.1 Dynamic and Output Equations

A number of outputs are needed to realize the desired co-design problem:

$$\mathbf{y} = [z_U, z_S, \ddot{z}_S, F, z_F, z_B^T, z_K^T]^T \quad (11)$$

namely, the unsprung mass position, sprung mass position, sprung mass acceleration, actuator force, actuator position, $n_b^{(i)}$ B-type component positions, and $n_k^{(i)}$ K-type component positions. The two sources or inputs are the force trajectory of the actuator F and the road velocity profile $\dot{\delta}$. Then the dynamics and output equations generated from the linearization of the programmatically-created model as described in Sec. 2.1 will have the following form:

$$\dot{\xi} = \mathbf{A}\xi + \mathbf{B}_f F + \mathbf{B}_\delta \dot{\delta} \quad (12a)$$

$$\mathbf{y} = \mathbf{C}\xi + \mathbf{D}_f F + \mathbf{D}_\delta \dot{\delta} \quad (12b)$$

noting that the matrices are dependent on the plant variables and problem parameters.

5.2 Objective

The co-design objective function will be the sum of several common performance metrics:

$$\Psi_d = \int_{t_0}^{t_f} (w_1 (y_1 - \delta)^2 + w_2 y_3^2 + w_3 y_4^2) dt \quad (13)$$

where the term $w_1 (y_1 - \delta)^2$ captures the *handling* performance, $w_2 y_3^2$ represents the passenger *comfort*, and $w_3 y_4^2$ control *effort* objective (see Refs. [15–17]). Combining Eqs. (12b) and (13) results in an LQDO objective function [28].

5.3 Constraints

Next, the states of the system are initialized to their zero equilibrium position with the following simple bound constraint:

$$\xi^{(i)}(t_0) = \mathbf{0} \quad (14)$$

To ensure that the separation between the sprung and unsprung masses remains tolerable, the following rattlespace constraint is necessary [3, 4, 15, 17, 18]:

$$|r| := |y_2 - y_1| \leq r_{\max} \quad (15)$$

Table 2 Co-design problem parameters.

Parameter	Value	Parameter	Value
t_0	0 s	t_f	3 s
m_{\min}	10^{-2} kg	m_{\max}	10^1 kg
b_{\min}	10^2 Ns/m	b_{\max}	10^5 Ns/m
k_{\min}	10^2 N/m	k_{\max}	10^6 N/m
r_{\max}	0.04 m	s_{\max}	0.04 m
m_U	65 kg	m_S	325 kg
w_1	$10^5 \text{ s}^{-1} \text{ m}^{-2}$	k_t	232.5×10^3 N/m
w_2	$0.5 \text{ s}^3 \text{ m}^{-2}$	b_t	0 Ns/m
w_3	$10^{-5} \text{ s}^{-1} \text{ N}^{-2}$		

This constraint can be converted into two linear constraints [28]. The LQDO problem class can readily handle linear inequality constraints unlike other solution strategies [17,28]. Similarly, stroke constraints are included on the 2-port components $\{F, B, K\}$ to ensure that their travel is within a tolerable level:

$$|y_5| \leq s_{\max} \quad (16a)$$

$$|y_{5+j}| \leq s_{\max} \quad j = 1, \dots, n_b^{(i)} + n_k^{(i)} \quad (16b)$$

Internal positioning constraints (i.e., constraints that ensure that all internal positions between U and S are properly ordered and between these masses) should also be included, but is currently left as future work. These constraints are essential when F is included in an architecture since the model for F ignores the velocity across it. To facilitate an easier visualization of the stroke constraints, we denote the largest magnitude all the stroke constraints as $S_{\max}(t)$.

All the previous constraints are necessary for the inner-loop problem using the nested co-design strategy. The outer-loop specific plant constraints are simple bounds on the linear coefficients [5,15,16]:

$$m_{\min} \leq m_j \leq m_{\max} \quad j = 1, \dots, n_m^{(i)} \quad (17a)$$

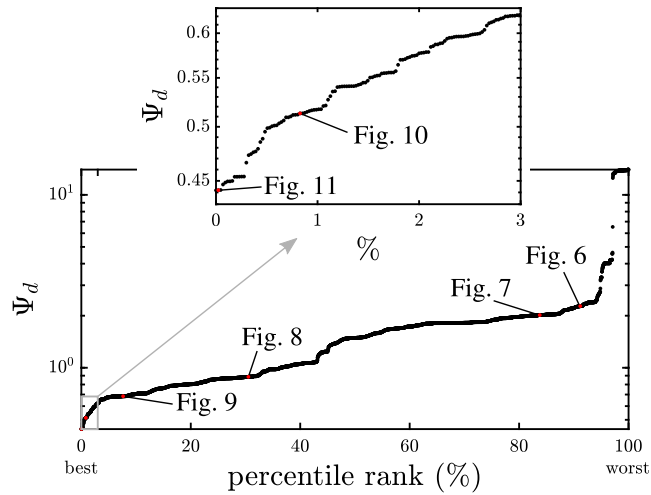
$$b_{\min} \leq b_j \leq b_{\max} \quad j = 1, \dots, n_b^{(i)} \quad (17b)$$

$$k_{\min} \leq k_j \leq k_{\max} \quad j = 1, \dots, n_k^{(i)} \quad (17c)$$

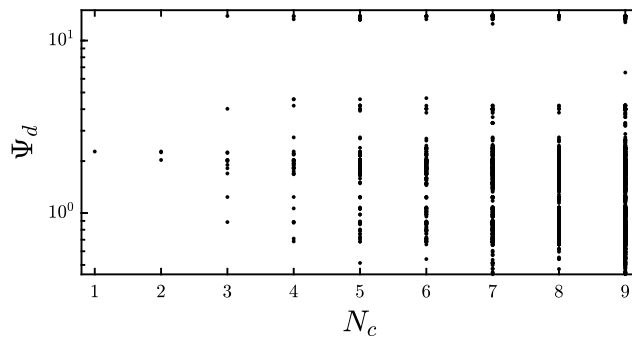
where the subscripts (m, b, k) indicate the additional mass, damper, and spring plant variables in the candidate architecture. While we are only using simple bounds in for the plant-specific constraints, a more comprehensive plant design formulation can be included in an LQDO-amenable co-design problem [28,31]. For example, we could instead design the springs based on their geometry [17,41].

6 CASE STUDY RESULTS

The problem parameters used in this study are shown in Table 2 and many are based on the study in Ref. [17]. A rough road input from Refs. [6,17] was used. With the component catalog and NSCs described in Sec. 4, there are 4,374 active suspension candidate architectures. For each of these suspension candidates, the optimal performance was determined by solving an automatically generated co-design problem specific to the candidate architecture. A number of software tools are linked in MATLAB in order to perform this task (and the code is available at Ref. [26]). The list of suspension architectures/graphs is generated using the code available in Ref. [37] as discussed in Sec. 3.2.1. Since the determination of the performance for each architecture can be completed independently, this task



(a) Performance vs. percentile rank.



(b) Performance vs. complexity.

Fig. 5 Summary of the results for 4,351 candidate suspensions.

is parallelized. The SIMSCAPE/SIMULINK dynamic models are automatically constructed and updated using custom code as discussed in Sec. 2.1. A combination of global (`patternsearch` with global search options) and local (`fmincon`) search algorithms are used to find solutions to Level \mathcal{P} . Finally, the Level C LQDO problem is solved using the code available at Ref. [39] as discussed in Sec. 2.2.

The results are summarized in Fig. 5 for 4,351 architectures. In Fig. 5(a), we see a large distribution for the performance results, including a select few that perform extremely poorly. For sixteen of the candidates, a feasible co-design solution could not be determined, but a more exhaustive search may lead to feasible solutions for these architectures. For seven of the architectures, the internal position constraints mentioned in Sec. 5.3 (which were not included in these results) were violated to an unacceptable degree producing unrealistically low values for Ψ_d , and therefore were removed from the results. Now, shown in Fig. 5(b) are the architectures stratified by the mechanical complexity metric in Eq. (10). In general, we observe that increasing the number of components can improve performance, but this trend only holds up to a certain point where additional complexity does not lead to better performance. However, there still are a large number of candidate architectures with large N_c that perform poorly. The complete set of results can be used to help determine if the increased mechanical complexity of a new candidate architecture is worth the performance improvement.

The results for a few candidate suspensions are shown in Table 3 and Figs. 6–11, including the pure active and canonical active suspensions. The best performing architecture with $N_c = 3$ is shown in Fig. 8, and is decidedly different than the canonical active architecture having the same number of components. In Fig. 9, the best performing architecture with $N_c = 4$ is shown. It is comprised out of

Table 3 Objective function, plant design, and maximum force for select suspensions.

Figure	Ψ_d	handling	comfort	effort	k_1	k_2	k_3	b_1	m_1	m_2	$\max(F)$
Fig. 6	2.32	1.00	0.42	0.89	—	—	—	—	—	—	528
Fig. 7	2.07	0.89	0.53	0.65	21.3	—	—	319	—	—	433
Fig. 8	0.91	0.51	0.13	0.27	14.1	—	—	—	3.8	—	265
Fig. 9	0.70	0.39	0.01	0.30	4.3	13.0	—	—	5.7	—	317
Fig. 10	0.52	0.30	0.07	0.15	38.3	11.7	—	—	2.8	10.0	250
Fig. 11	0.45	0.24	0.02	0.20	14.1	15.8	4.6	100	8.9	2.2	409

* All k have units of kN/m, b have units of Ns/m, m have units of kg, and F have units of N.

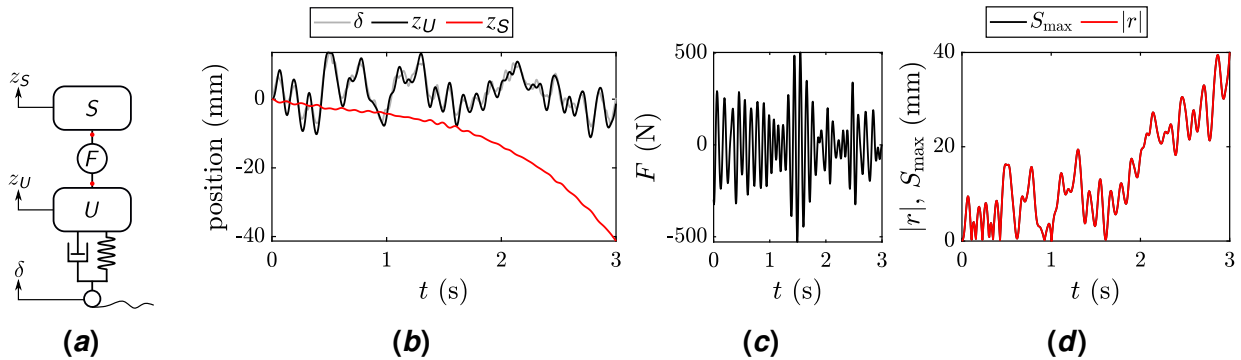


Fig. 6 Results for the pure active architecture ($N_c = 1$): (a) architecture; (b) positions; (c) control; (d) rattlespace and stroke limits.

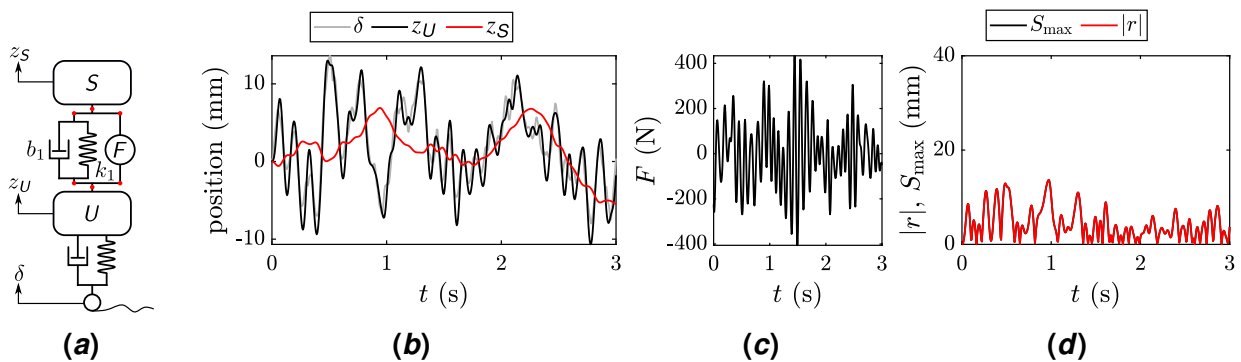


Fig. 7 Results for the canonical active architecture ($N_c = 3$): (a) architecture; (b) positions; (c) control; (d) rattlespace and stroke limits.

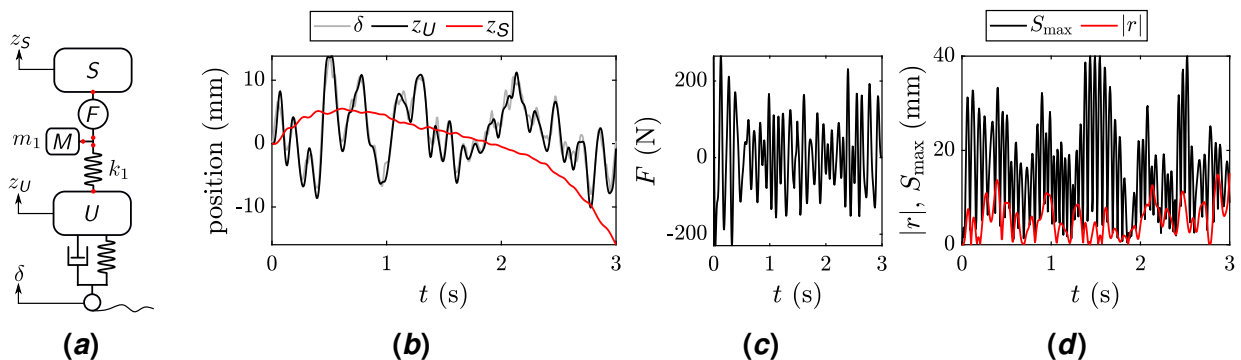


Fig. 8 Results for best performing architecture with $N_c = 3$: (a) architecture; (b) positions; (c) control; (d) rattlespace and stroke limits.

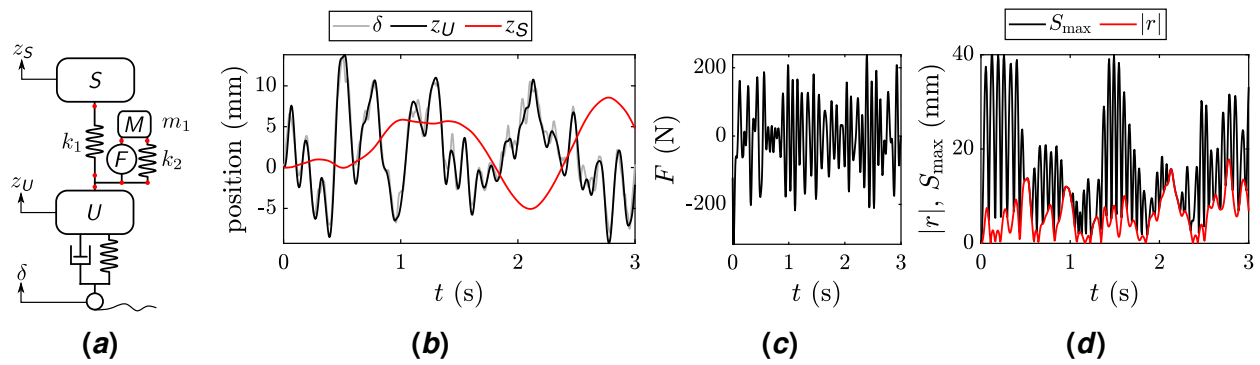


Fig. 9 Results for best performing architecture with $N_c = 4$: (a) architecture; (b) positions; (c) control; (d) rattlespace and stroke limits.

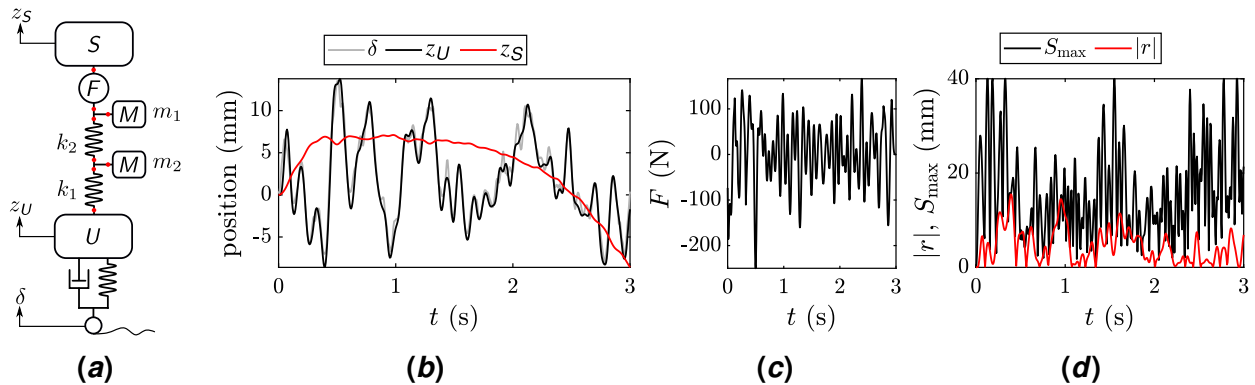


Fig. 10 Results for best performing architecture with $N_c = 5$: (a) architecture; (b) positions; (c) control; (d) rattlespace and stroke limits.

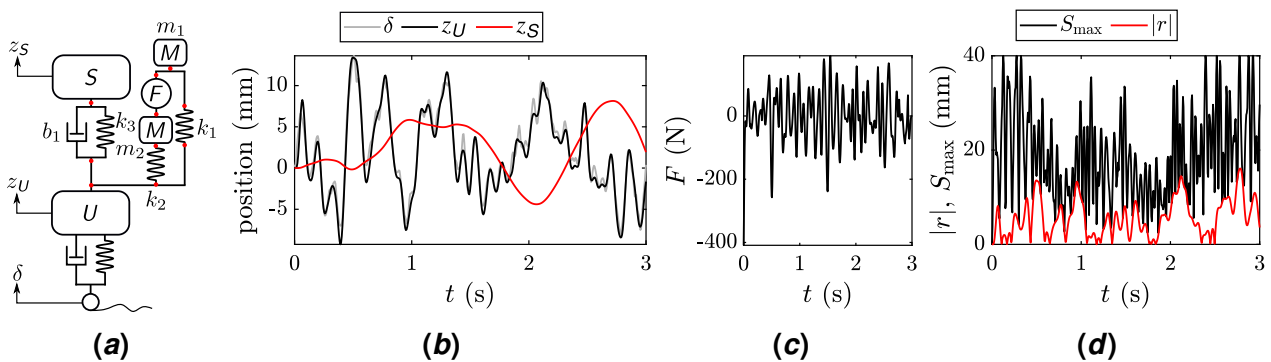


Fig. 11 Results for best performing architecture with $N_c = 7$: (a) architecture; (b) positions; (c) control; (d) rattlespace and stroke limits.

two springs and one additional mass and resembles the dynamic absorber architecture in Fig. 1(d). The primary difference between these architectures is that the force actuator is attached to the additional mass rather than between U and S . Finally, the best architectures for $N_c = 5$ and $N_c = 7$ are shown in Figs. 10 and 11, respectively. The best architecture for $N_c = 6$ is not shown as there is no performance improvement over a less mechanically complex architecture.

Comparing the performance measures, the value of Ψ_d is much lower for the other architectures than for the canonical active suspension ($4.6\times$ lower in Fig. 11); thus there seems to be a large amount of improvement available if we consider architecture changes in the vehicle suspension domain. Qualitatively observing the position profiles of z_U and z_S in Figs. 6–11, we see a general smoothing of z_S as well as a better agreement between δ and z_U for the suspensions with a lower value of Ψ_d . For all the shown architectures, except the canonical active, the stroke limit is reached during some part of the time horizon, hence the value of the stroke inequality constraints in our problem formulation. The individual parts of the objective function in Eq. (13) are also shown in Table 3. While Fig. 9 has the lowest overall objective function value, Fig. 9 has the lowest comfort objective part and Fig. 10 has the lowest control effort objective part of the shown architectures. Determining the solution to multiobjective problems will add further complexity to the design problem formulation and increased evaluation cost. It is up to further design activities to determine if the identified suspensions can satisfy other necessary design requirements that we have not considered here.

Many of the architectures have issues related to the internal positioning constraints, and thus, are not physically realizable. One of these architectures is shown in Fig. 10, where the relative positions of the springs switch during the time horizon. The primary cause of this issue is the ideal force source model for F , but other factors such as low spring stiffness can also cause overlapping elements in the suspension. Such issues with the modeling of the system were only identified during the analysis of the preliminary results. Performing this kind of architecture study can reveal representation and modeling issues that are not necessary to consider when only operating on the canonical architecture realizations.

The results were obtained using a computer with an Intel Xeon Gold 6130 CPU @ 2.10 GHz, 64 GB DDR4-2666 RAM, WINDOWS 10 64-bit, and MATLAB 2018a. The total time needed to generate all 4374 graphs was 0.15 hr. The average time to solve the co-design problem for a single architecture was 0.8 thread-hr (and a total of 73.1 hours using 48 threads). As noted previously, evaluating the co-design problems is an easily parallelizable task so multiple machines or a cluster could be used to decrease the absolute computation time.

7 DISCUSSION

There are some notable differences between the considered vehicle suspension design methodology and passive vehicle suspensions synthesis methods mentioned in Sec. 1. The primary difference is the modifications required when dealing with an active versus passive system. The evaluation of passive systems lends itself well towards analysis in the frequency domain [7–11]. However, time-domain methods are required when the path constraints in Eq. (3d) are necessary, which are required when F is present. Furthermore, time-domain methods are effective when LQDO with open-loop control is preferable to determine the system performance limits or insights into the final control-system embodiment. Frequency-based metrics, such as suspension quality and control input spectral density, are applicable to active suspensions but require assumptions on the control scheme such as linear feedback [15, 16].

Frequency-domain methods have a considerable number of advantages including the ability to capture effectively general properties of the system over a variety of conditions. In addition, there is extensive existing theory available for such systems that integrates well into the control design phase. A number of authors working with passive suspensions have focused on synthesis through the realization of real-rational functions of a certain degree [7, 8, 10]. Under certain assumptions, methods from

electrical circuit synthesis such as the Brune or Bott–Duffin methods can construct a passive, lumped network that matches the desired transfer function [8, 42]. However, these methods can have issues with non-minimality and can require ideal transformers (levers in the mechanical system) [11, 43]. Specific architectures have been identified that facilitate design activities around more useful architectures (without transformers), but they are limited in complexity and not all forms can be realized [43].

In summary, the traditional frequency-domain synthesis approaches are limited in their ability to minimize complexity and generalize to new synthesis problems. The component catalog approach in Eq. (9) and general graph-based representation of the architectures from Ref. [34] provides a designer with the freedom to control directly the contents and complexity of the candidate architectures. This includes components selection, number of P -type components, and many other network-based metrics. Most of the previous suspension synthesis approaches allow only inerters, not general 1-port mass components, so the dynamic absorbers from Fig. 1 would not be obtainable. If we remove the requirement that F is present in all candidate architectures, we can also synthesize passive suspensions. In general, we are now constrained to the allowable graphs versus the allowable transfer functions.

There are other advantages of the proposed approach from a design problem representation viewpoint. The proposed design optimization framework allows for more desirable parameterization of the plant design. For example, we can readily include direct bounds on all of the components such as in Eq. (17) or even more general parameterizations such as the geometry of the spring [17]. Other relevant factors, such as cost metrics, can also be considered in the co-design problem.

Switching to the general design methodology, the area of hybrid electric vehicle powertrain design has investigated \mathcal{APC} problems [44, 45]. In Ref. [44], the authors propose a similar trilevel solution approach, but their work focuses on the challenges specific to their application area rather than the domain-agnostic view taken here. Here, the goal is not to define and solve general \mathcal{APC} design problems but rather a specific form where effective tools/methods are available and are relevant to design engineers (such as the presented vehicle suspension case study). Defining an optimization problem class in this manner based on available solution methods is not uncommon. Dynamic optimization with either LQDO or the nonlinear form is a prime example where discussing the tradeoffs between the linear and nonlinear forms is critical *because* of the effective solution strategies. Understanding if your design goals are met by a particular problem class is up to the designer as there are tradeoffs between problem efficacy, computational cost, and more. In many aspects, the described \mathcal{APC} problem class captures the simplest cases applicable to graph-representable, dynamic engineering systems. Even small deviations from the proposed problem class could result in rampant growth in its evaluation cost. In contrast, there may be alternatives to the proposed trilevel solution approach that could prove to be more computationally efficient or generally applicable. Some of these variations are now described.

The nonlinear constitutive relations can be captured by the enumeration approach in Ref. [37] assuming models can be appropriately constructed from undirected edges. A key consideration is still the need for an explicit derivative function (consideration 5). Constructing a simulation-based model is typically not satisfactory for many of the numerical methods needed to efficiently solve the co-design problem [46]. An example of an alternative graph-based modeling approach is presented in Ref. [47] and is applicable to fluid-based thermal systems. Given a graph-based architecture specification, the explicit bilinear derivative function can be constructed (so these models do not fit within the purview of LQDO). OPTIMICA is another tool that may facilitate modeling and optimization for the problem class of interest [48].

If we instead require general co-design problems for Prob. (8) rather than LQDO-amenable co-design problems, the simultaneous co-design strategy could be more efficient in some cases, and may avoid potential infeasibility issues associated with \mathcal{I} [30]. There are a number of tools available to solve the resulting nonlinear dynamic optimization such as GPOPS-II [49]. There are also many interesting architecture design problems without plant or control systems, such Levels \mathcal{A}/\mathcal{P} for passive analog

circuit synthesis [28] or Levels $\mathcal{A}/(C/D)$ for fluid-based thermal circuits [50].

In Level \mathcal{A} , there are a number of alternatives to the brute-force generation procedure used here including constraint logic programming and other custom algorithms [51–55]. There are also alternatives to enumeration. Semi-optimal, heuristic-based methods for solving the combinatorial problem have included graph grammars [56], A-design [57], evolutionary computation [58, 59], simulated annealing [60], or machine learning techniques [61]. If enumeration is not possible, then these methods could be effective alternatives. Going beyond enumeration is essential for attempting to find solutions to large \mathcal{APC} problems.

With some of these approaches, both architecture and plant design can be solved for simultaneously [58], although some argue in favor of the nested approach for certain problems [59]. In the hybrid electric vehicle design, many argue for the nested approach in their co-design problems [44, 45].

8 CONCLUSION

In this article, a problem class with combined architecture, plant, and control design was described. Achieving successful design automation in this class of problems requires adequate theory and tools to support such considerable scope and complexity. The select problem class leverages a number of existing theory and tools and is particularly effective due to the symbiosis between labeled graph representations of architectures, dynamic models constructed from linear physical elements, linear-quadratic dynamic optimization, and the nested co-design solution strategy. However, even with the proposed problem structure, there will continue to be challenges associated with the combinatorial nature of the architecture design, nonconvexity and feasibility of general co-design problems, and infinite-dimensional nature of dynamic optimization problems.

A combined architecture, plant, and control design problem in the described problem class was posed for a vehicle suspension application, and is an area where a limited set of active architectures have been considered previously. All 4,374 candidate suspensions were evaluated through an automatically constructed co-design problem. The results demonstrated that changes to the vehicle suspension architecture can result in improved performance, but at the cost of increased mechanical complexity.

It remains future work to study the effectiveness of the proposed approach including inerters for passive vehicle suspension synthesis and compare the results to some of the existing literature [7–11]. Moreover, there are a number of improvements that can be made to the problem formulation. The inclusion of the internal positioning constraints is essential to ensure that many of the results are physically meaningful. Multiple road inputs can also be considered simultaneously to give a better representation of all the environments in which the suspension will need to function as well as sensitivity to other problem parameters. Finally, frequency domain properties, such as suspension quality spectral density and control energy spectral density, could also be utilized for a more effective problem formulation [15]. Such design formulation advancements could push the direct outcomes of additional \mathcal{APC} design studies towards novel and realizable vehicle suspension systems.

REFERENCES

- [1] Kasturi, P., and Dupont, P., 1998. “Constrained optimal control of vibration dampers”. *Journal of Sound and Vibration*, **215**(3), Aug., pp. 499–509. doi: [10.1006/jsvi.1998.1661](https://doi.org/10.1006/jsvi.1998.1661)
- [2] Hrovat, D., 1997. “Survey of advanced suspension developments and related optimal control applications”. *Automatica*, **33**(10), Oct., pp. 1781–1817. doi: [10.1016/S0005-1098\(97\)00101-5](https://doi.org/10.1016/S0005-1098(97)00101-5)

- [3] Hrovat, D., 1993. “Applications of optimal control to advanced automotive suspension design”. *ASME Journal of Dynamic Systems, Measurement, and Control*, **115**(2B), June, pp. 328–342. doi: [10.1115/1.2899073](https://doi.org/10.1115/1.2899073)
- [4] Gobbi, M., and Mastinu, G., 2001. “Analytical description and optimization of the dynamic behaviour of passively suspended road vehicles”. *Journal of Sound and Vibration*, **245**(3), Aug., pp. 457–481. doi: [10.1006/jsvi.2001.3591](https://doi.org/10.1006/jsvi.2001.3591)
- [5] He, Y., and McPhee, J., 2005. “Multidisciplinary design optimization of mechatronic vehicles with active suspensions”. *Journal of Sound and Vibration*, **283**(1-2), May, pp. 217–241. doi: [10.1016/j.jsv.2004.04.027](https://doi.org/10.1016/j.jsv.2004.04.027)
- [6] Allison, J. T., 2008. “Optimal partitioning and coordination decisions in decomposition-based design optimization”. Ph.D. dissertation, The University of Michigan, Ann Arbor, MI, USA, May. url: <http://hdl.handle.net/2027.42/58449>
- [7] Chen, M. Z. Q., Papageorgiou, C., Scheibe, F., Wang, F.-c., and Smith, M., 2009. “The missing mechanical circuit element”. *IEEE Circuits and Systems Magazine*, **9**(1), pp. 10–26. doi: [10.1109/MCAS.2008.931738](https://doi.org/10.1109/MCAS.2008.931738)
- [8] Chen, M. Z. Q., Hu, Y., and Wang, F.-C., 2015. “Passive mechanical control with a special class of positive real controllers: Application to passive vehicle suspensions”. *Journal of Dynamic Systems, Measurement, and Control*, **137**(12), Oct., p. 121013. doi: [10.1115/1.4031630](https://doi.org/10.1115/1.4031630)
- [9] Papageorgiou, C., and Smith, M., 2006. “Positive real synthesis using matrix inequalities for mechanical networks: Application to vehicle suspension”. *IEEE Transactions on Control Systems Technology*, **14**(3), May, pp. 423–435. doi: [10.1109/TCST.2005.863663](https://doi.org/10.1109/TCST.2005.863663)
- [10] Smith, M. C., 2002. “Synthesis of mechanical networks: The inerter”. *IEEE Transactions on Automatic Control*, **47**(10), Oct., pp. 1648–1662. doi: [10.1109/TAC.2002.803532](https://doi.org/10.1109/TAC.2002.803532)
- [11] Wang, F.-C., and Chan, H.-A., 2011. “Vehicle suspensions with a mechatronic network strut”. *Vehicle System Dynamics*, **49**(5), Dec., pp. 811–830. doi: [10.1080/00423111003797143](https://doi.org/10.1080/00423111003797143)
- [12] Deshmukh, A. P., Herber, D. R., and Allison, J. T., 2015. “Bridging the gap between open-loop and closed-loop control in co-design: A framework for complete optimal plant and control architecture design”. In American Control Conference, pp. 4916–4922. doi: [10.1109/ACC.2015.7172104](https://doi.org/10.1109/ACC.2015.7172104)
- [13] Koch, G., and Kloiber, T., 2014. “Driving state adaptive control of an active vehicle suspension system”. *IEEE Transactions on Control Systems Technology*, **22**(1), Jan., pp. 44–57. doi: [10.1109/tcst.2013.2240455](https://doi.org/10.1109/tcst.2013.2240455)
- [14] Bourmistrova, A., Storey, I., and Subic, A., 2005. “Multiobjective optimisation of active and semi-active suspension systems with application of evolutionary algorithm”. In International Conference on Modelling and Simulation, pp. 1217–1223.
- [15] Fathy, H. K., Papalambros, P. Y., Ulsoy, A. G., and Hrovat, D., 2003. “Nested plant/controller optimization with application to combined passive/active automotive suspensions”. In American Control Conference, Vol. 4, pp. 3375–3380. doi: [10.1109/ACC.2003.1244053](https://doi.org/10.1109/ACC.2003.1244053)
- [16] Alyaqout, S. F., Papalambros, P. Y., and Ulsoy, A. G., 2007. “Combined design and robust control of a vehicle passive/active suspension”. In European Control Conference, pp. 1264–1270.
- [17] Allison, J. T., Guo, T., and Han, Z., 2014. “Co-design of an active suspension using simultaneous dynamic optimization”. *ASME Journal of Mechanical Design*, **136**(8), June, p. 081003. doi: [10.1115/1.4027335](https://doi.org/10.1115/1.4027335)
- [18] Ulsoy, A. G., Hrovat, D., and Tseng, T., 1994. “Stability robustness of LQ and LQG active suspensions”. *Journal of Dynamic Systems, Measurement, and Control*, **116**(1), Mar., pp. 123–131. doi: [10.1115/1.2900666](https://doi.org/10.1115/1.2900666)
- [19] Borutzky, W., 2010. *Bond Graph Methodology*, 1st ed. Springer. doi: [10.1007/978-1-84882-882-7](https://doi.org/10.1007/978-1-84882-882-7)
- [20] Kypuros, J. A., 2013. *System Dynamics and Control with Bond Graph Modeling*. CRC Press.
- [21] Karnopp, D. C., Margolis, D. L., and Rosenberg, R. C., 2012. *System Dynamics: Modeling*,

Simulation, and Control of Mechatronic Systems, 5th ed. Wiley.

- [22] Gonzalez, G., and Galindo, R., 2008. “Removing the algebraic loops of a bond graph model”. *Proceedings of the Institution of Mechanical Engineers, Part I: Journal of Systems and Control Engineering*, **222**(6), Sept., pp. 543–556. doi: [10.1243/09596518jsce559](https://doi.org/10.1243/09596518jsce559)
- [23] Maschke, B. M., and Villarroja, M., 1995. “Properties of descriptor systems arising from bond graph models”. *Mathematics and Computers in Simulation*, **39**(5–6), Nov., pp. 491–497. doi: [10.1016/0378-4754\(95\)00109-1](https://doi.org/10.1016/0378-4754(95)00109-1)
- [24] Cellier, F. E., and Nebot, A., 2005. “The Modelica bond graph library”. In International Modelica Conference, pp. 57–65.
- [25] Wu, Z., Campbell, M. I., and Fernández, B. R., 2008. “Bond graph based automated modeling for computer-aided design of dynamic systems”. *ASME Journal of Mechanical Design*, **130**(4), Apr., p. 041102. doi: [10.1115/1.2885180](https://doi.org/10.1115/1.2885180)
- [26] Herber, D. R., and Allison, J. T., 2018. PM suspensions. GitHub. url: <https://github.com/danielrherber/pm-suspensions>
- [27] The MathWorks. linearize. Accessed on 3/3/2018. url: <https://www.mathworks.com/help/slcontrol/ug/linearize.html>
- [28] Herber, D. R., 2017. “Advances in combined architecture, plant, and control design”. Ph.D. dissertation, University of Illinois at Urbana-Champaign, Urbana, IL, USA, Dec. url: <https://www.ideals.illinois.edu/handle/2142/99394>
- [29] Fathy, H. K., Reyer, J. A., Papalambros, P. Y., and Ulsoy, A. G., 2001. “On the coupling between the plant and controller optimization problems”. In American Control Conference, Vol. 3, pp. 1864–1869. doi: [10.1109/ACC.2001.946008](https://doi.org/10.1109/ACC.2001.946008)
- [30] Herber, D. R., and Allison, J. T., 2018. “Nested and simultaneous solution strategies for general combined plant and control design problems”. *ASME Journal of Mechanical Design*, **141**(1), Jan., p. 011402. doi: [10.1115/1.4040705](https://doi.org/10.1115/1.4040705)
- [31] Chilan, C. M., Herber, D. R., Nakka, Y. K., Chung, S.-J., Allison, J. T., Aldrich, J. B., and Alvarez-Salazar, O. S., 2017. “Co-design of strain-actuated solar arrays for spacecraft precision pointing and jitter reduction”. *AIAA Journal*, **55**(9), Sept., pp. 3180–3195. doi: [10.2514/1.J055748](https://doi.org/10.2514/1.J055748)
- [32] Deshmukh, A. P., and Allison, J. T., 2016. “Multidisciplinary dynamic optimization of horizontal axis wind turbine design”. *Structural and Multidisciplinary Optimization*, **53**(1), Jan., pp. 15–27. doi: [10.1007/s00158-015-1308-y](https://doi.org/10.1007/s00158-015-1308-y)
- [33] Lawler, E. L., 1976. *Combinatorial Optimization: Networks and Matroids*. Holt, Rinehart and Winston.
- [34] Herber, D. R., Guo, T., and Allison, J. T., 2017. “Enumeration of architectures with perfect matchings”. *ASME Journal of Mechanical Design*, **139**(5), Apr., p. 051403. doi: [10.1115/1.4036132](https://doi.org/10.1115/1.4036132)
- [35] Rispoli, F. J., 2007. *Applications of Discrete Mathematics*, updated ed. McGraw-Hill, ch. Applications of Subgraph Enumeration.
- [36] Wyatt, D. F., Wynn, D. C., Jarrett, J. P., and Clarkson, P. J., 2011. “Supporting product architecture design using computational design synthesis with network structure constraints”. *Research in Engineering Design*, **23**(1), Apr., pp. 17–52. doi: [10.1007/s00163-011-0112-y](https://doi.org/10.1007/s00163-011-0112-y)
- [37] Herber, D. R., Guo, T., and Allison, J. T., 2016. PM architectures project. GitHub. url: <https://github.com/danielrherber/pm-architectures-project>
- [38] Herber, D. R., and Allison, J. T., 2017. Enhancements to the perfect matching-based tree algorithm for generating architectures. Technical report UIUC-ESDL-2017-02, Engineering System Design Lab, Urbana, IL, USA, Dec. url: <https://ideals.illinois.edu/handle/2142/98990>
- [39] Herber, D. R., Lee, Y. H., and Allison, J. T., 2017. DT QP project. GitHub. url: <https://github.com/danielrherber/dt-qp-project>
- [40] Smith, M. C., and Wang, F.-C., 2004. “Performance benefits in passive vehicle suspen-

- sions employing inerters”. *Vehicle System Dynamics*, **42**(4), Dec., pp. 235–257. doi: [10.1080/00423110412331289871](https://doi.org/10.1080/00423110412331289871)
- [41] Liu, T., Azarm, S., and Chopra, N., 2017. “On decentralized optimization for a class of multisub-system codesign problems”. *ASME Journal of Mechanical Design*, **139**(12), Oct., p. 121404. doi: [10.1115/1.4037893](https://doi.org/10.1115/1.4037893)
- [42] Anderson, B. D. O., and Vongpanitlerd, S., 1973. *Network Analysis and Synthesis: A Modern Systems Theory Approach*. Prentice-Hall.
- [43] Chen, M. Z. Q., and Smith, M. C., 2008. “Electrical and mechanical passive network synthesis”. In *Recent Advances in Learning and Control*, V. D. Blondel, S. P. Boyd, and H. Kimura, eds., Vol. 371. Springer, pp. 35–50. doi: [10.1007/978-1-84800-155-8_3](https://doi.org/10.1007/978-1-84800-155-8_3)
- [44] Silvas, E., Hofman, T., Murgovski, N., Etman, P., and Steinbuch, M., 2017. “Review of optimization strategies for system-level design in hybrid electric vehicles”. *IEEE Transactions on Vehicular Technology*, **66**(1), Jan., pp. 57–70. doi: [10.1109/tvt.2016.2547897](https://doi.org/10.1109/tvt.2016.2547897)
- [45] Bayrak, A. E., Kang, N., and Papalambros, P. Y., 2016. “Decomposition-based design optimization of hybrid electric powertrain architectures: simultaneous configuration and sizing design”. *ASME Journal of Mechanical Design*, **138**(7), June, p. 071405. doi: [10.1115/1.4033655](https://doi.org/10.1115/1.4033655)
- [46] Allison, J. T., and Herber, D. R., 2014. “Multidisciplinary design optimization of dynamic engineering systems”. *AIAA Journal*, **52**(4), Apr., pp. 691–710. doi: [10.2514/1.J052182](https://doi.org/10.2514/1.J052182)
- [47] Koeln, J. P., Williams, M. A., Pangborn, H. C., and Alleyne, A. G., 2016. “Experimental validation of graph-based modeling for thermal fluid power flow systems”. In ASME Dynamic Systems and Control Conference, no. DSCC2016-9782, p. V002T21A008. doi: [10.1115/DSCC2016-9782](https://doi.org/10.1115/DSCC2016-9782)
- [48] Åkesson, J., 2008. “Optimica—An extension of modelica supporting dynamic optimization”. In International Modelica Conference, pp. 57–66.
- [49] Patterson, M. A., and Rao, A. V., 2014. “GPOPS-II: A MATLAB software for solving multiple-phase optimal control problems using hp-adaptive gaussian quadrature collocation methods and sparse nonlinear programming”. *ACM Transactions on Mathematical Software*, **41**(1), Oct., pp. 1–37. doi: [10.1145/2558904](https://doi.org/10.1145/2558904)
- [50] Peddada, S. R. T., Herber, D. R., Pangborn, H. C., Alleyne, A. G., and Allison, J. T., 2018. “Optimal flow control and single split architecture exploration for fluid-based thermal management”. In ASME International Design Engineering Technical Conferences, no. DETC2018-86148, p. V02AT03A005. doi: [10.1115/DETC2018-86148](https://doi.org/10.1115/DETC2018-86148)
- [51] Silvas, E., Hofman, T., Serebrenik, A., and Steinbuch, M., 2015. “Functional and cost-based automatic generator for hybrid vehicles topologies”. *IEEE/ASME Transactions on Mechatronics*, **20**(4), Aug., pp. 1561–1572. doi: [10.1109/tmech.2015.2405473](https://doi.org/10.1109/tmech.2015.2405473)
- [52] Münzer, C., Helms, B., and Shea, K., 2013. “Automatically transforming object-oriented graph-based representations into boolean satisfiability problems for computational design synthesis”. *ASME Journal of Mechanical Design*, **135**(10), July, p. 101001. doi: [10.1115/1.4024850](https://doi.org/10.1115/1.4024850)
- [53] Snavely, G. L., and Papalambros, P. Y., 1993. “Abstraction as a configuration design methodology”. In *Advances in Design Automation*, Vol. 65, pp. 297–305.
- [54] Faulon, J.-L., Churchwell, C. J., and Visco, D. P., 2003. “The signature molecular descriptor. 2. Enumerating molecules from their extended valence sequences”. *Journal of Chemical Information and Computer Sciences*, **43**(3), May, pp. 721–734. doi: [10.1021/ci020346o](https://doi.org/10.1021/ci020346o)
- [55] Bayrak, A. E., Ren, Y., and Papalambros, P. Y., 2016. “Topology generation for hybrid electric vehicle architecture design”. *ASME Journal of Mechanical Design*, **138**(8), June, p. 081401. doi: [10.1115/1.4033656](https://doi.org/10.1115/1.4033656)
- [56] Schmidt, L. C., Shetty, H., and Chase, S. C., 2000. “A graph grammar approach for structure synthesis of mechanisms”. *ASME Journal of Mechanical Design*, **122**(4), Dec., pp. 371–376. doi: [10.1115/1.1315299](https://doi.org/10.1115/1.1315299)

- [57] Campbell, M. I., Cagan, J., and Kotovsky, K., 2000. “Agent-based synthesis of electromechanical design configurations”. *ASME Journal of Mechanical Design*, **122**(1), Mar., pp. 61–69. doi: [10.1115/1.533546](https://doi.org/10.1115/1.533546)
- [58] Das, A., and Vemuri, R., 2007. “An automated passive analog circuit synthesis framework using genetic algorithms”. In IEEE Computer Society Annual Symposium on VLSI. doi: [10.1109/ISVLSI.2007.22](https://doi.org/10.1109/ISVLSI.2007.22)
- [59] Grimbey, J. B., 2000. “Automatic analogue circuit synthesis using genetic algorithms”. *IEE Proceedings - Circuits, Devices and Systems*, **147**(6), Dec., pp. 319–323. doi: [10.1049/ip-cds:20000770](https://doi.org/10.1049/ip-cds:20000770)
- [60] Ochotta, E. S., Rutenbar, R. A., and Carley, L. R., 1996. “Synthesis of high-performance analog circuits in ASTRX/OBLX”. *IEEE Transactions on Computer-Aided Design of Integrated Circuits and Systems*, **15**(3), Mar., pp. 273–294. doi: [10.1109/43.489099](https://doi.org/10.1109/43.489099)
- [61] Guo, T., Herber, D. R., and Allison, J. T., 2018. “Reducing evaluation cost for circuit synthesis using active learning”. In ASME International Design Engineering Technical Conferences, no. DETC2018-85654, p. V02AT03A011. doi: [10.1115/DETC2018-85654](https://doi.org/10.1115/DETC2018-85654)

A LEVEL \mathcal{P} CONVEXITY OF THE VEHICLE SUSPENSION CO-DESIGN PROBLEMS

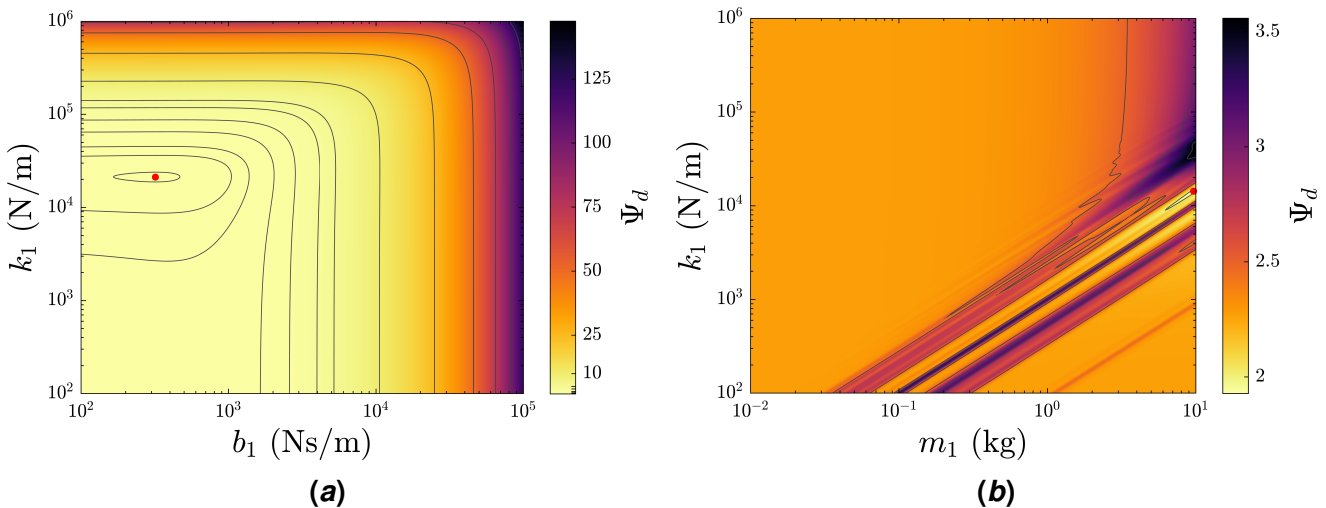


Fig. 12 The objective-plant space for two candidate architectures with two plant variables with the minimum marked with a circle: (a) convex behavior for Fig. 7(a); (b) nonconvex behavior for Fig. 8(a).

As described in Ref. [29] and explicitly shown in Ref. [30], even simple co-design problems can have nonconvex outer loops. Understanding the nature of the nonconvexity in a particular optimization problem can provide much guidance when seeking global solutions. Due to the nature of the described \mathcal{APC} problems, entire sets of co-design problems need to be accounted for in order to develop an effective automated optimization procedure in Levels $\mathcal{P}/(C/D)$. This a challenging proposition. In this study, this means 4,351 co-design problems, one for each suspension. A few candidate architectures were studied to help determine the global optimization tuning parameters. In Fig. 12, the objective-plant space (i.e., the space explored in the outer loop of the nested co-design strategy) is shown for the canonical active suspension (see Fig. 1(c)) and dynamic absorber without the additional damper (see Fig. 1(d)). Note that Fig. 12(a) is seemingly convex, while Fig. 12(b) is noisy and nonconvex. Some

of the numerical noise is due to the discretization chosen for implementation of the direct transcription method.